

# Detection of incipient rubber particle cavitation in toughened PMMA using dynamic mechanical tests

C.B. Bucknall<sup>a,\*</sup>, R. Rizzieri<sup>a</sup>, D.R. Moore<sup>b</sup>

<sup>a</sup>Advanced Materials Department, Cranfield University, Bedford MK43 0AL, UK

<sup>b</sup>ICI R&T Group, Wilton, Middlesbrough, Cleveland TS90 8JE, UK

Received 7 June 1999; received in revised form 23 July 1999; accepted 2 September 1999

---

## Abstract

Dynamic mechanical measurements were carried out on rubber-toughened poly(methyl methacrylate) (RT-PMMA) under superimposed static tensile and compressive stresses, in the temperature range  $-40$  to  $10^{\circ}\text{C}$ , which includes the glass transition of the rubber phase. Under compression, where the dynamic loss curves were very reproducible, the  $\tan \delta$  peak due to the rubber particles shifted to higher temperatures with increasing superimposed stress. Under tension, by contrast, the loss curves were much more variable, in some cases splitting into two peaks, and the peak temperature was no longer a function of the superimposed stress. This behaviour is consistent with incipient cavitation in a proportion of rubber particles under tensile stress. It is concluded that the transition from reproducible to variable dynamic mechanical behaviour marks the onset of cavitation in the rubber phase. The specimen-to-specimen variations observed under superimposed tension appear to be due to differences in strain distributions within and between rubber particles. The procedure provides a method for measuring the resistance of rubber particles to cavitation in response to mechanically and thermally generated stresses, and for distinguishing the cavitation event from subsequent dilatational yielding. © 2000 Elsevier Science Ltd. All rights reserved.

**Keywords:** Rubber toughening; Cavitation; Dynamic mechanical properties

---

## 1. Introduction

The fracture resistance of rubber-toughened plastics is now known to be critically dependent upon void formation in the rubber phase [1,2]. In most types of toughened plastics, cavitation of the rubber particles near a crack tip is followed by shear yielding in the intervening matrix to form *dilatation bands*, thereby allowing the material to yield at greatly reduced stresses. There is also a growing body of evidence to show that rubber particle cavitation is a necessary precursor to multiple crazing in toughened glassy polymers such as ABS and high-impact polystyrene (HIPS) [3]. In view of these developments, it is clearly important to develop a quantitative understanding of the factors controlling cavitation of the rubber phase. In order to do so, it is necessary to distinguish between the cavitation event itself and the dilatational yielding that often accompanies it. The present study addresses this problem.

Void formation in the rubber phase requires an input of energy, which is supplied by a combination of differential thermal contraction and mechanical loading. In toughened thermoplastics, volume strains in the order of 1% are

generated within the rubber particles simply on cooling from the  $T_g$  of the matrix (typically  $>100^{\circ}\text{C}$ ) to  $23^{\circ}\text{C}$  [4]. Application of tensile stress produces additional dilatational volume strains of a similar magnitude in the rubber particles. These strains are partially or fully released when the particles cavitate. Under appropriate conditions, differential thermal contraction alone can be sufficient to cause cavitation, as demonstrated by Morbitzer et al. in dynamic mechanical studies on ABS [5,6]. Their work concentrated on the secondary loss peak at about  $-90^{\circ}\text{C}$ , which is due to the glass transition of polybutadiene. It showed that under certain conditions, in the absence of superimposed axial loading, the secondary loss peak splits into two, with maxima up to  $15^{\circ}\text{C}$  apart. The first loss maximum, on the low temperature side of the double peak, is obviously due to intact particles, which are able to relax rapidly because of the increased free volume due to constraints on thermal contraction. Morbitzer et al. attributed the second maximum to debonded particles, but in the light of more recent work it is clear that at least some of the observed shifts are due to *internal* cavitation of the rubber phase. Their studies showed that cavitation and/or debonding are promoted by low levels of grafting [5], the presence of added liquids [6], increases in particle size, and reductions in the rubber

---

\* Corresponding author.

content. As the volume fraction of rubber particles is reduced, the matrix imposes increasing constraints upon their thermal contraction, and the resulting internal stresses and enhancement of free volume in the rubber phase cause a downward shift in peak temperature, until the local strain energy reaches a critical value and the particles cavitate.

In recent years, the development of an energy-balance model has led to an improved quantitative understanding of the cavitation process [1–4,7,9]. Void formation is made possible by the release of energy stored in the rubber particle itself (as volume strain energy) and in the surrounding rigid matrix. As noted earlier, both differential thermal contraction and mechanical loading contribute to the available stored energy [4], which is also affected by rubber content and particle size [8]. Cavitation occurs when the energy released during expansion of the voids is sufficient for both the formation of new surface and associated stretching of the surrounding rubber. Particle size is important because surface-to-volume ratios increase as length scales are reduced. The energy required for cavitation depends on the shear modulus of the rubber phase, which determines the amount of work done in stretching the rubber to accommodate the void. Another important factor is the surface energy of the rubber, which can be reduced by adding suitable liquids. This might explain the observations of Morbitzer et al. [6] on the effects of liquids on the dynamic mechanical behaviour of ABS. The total surface area generated during the cavitation of any given particle depends upon the number, shape and size distribution of the voids contributing to that expansion. Recent studies indicate that cavitation in toughened plastics often involves the formation of several voids within each rubber particle, and that calculations based on the formation of one void per particle simply define a lower limit on conditions for cavitation [10]. For this reason, rubber particles may prove much more difficult to cavitate than is predicted by the original energy-balance model.

The present study is based upon earlier work by Lin et al. [11], who used dynamic mechanical tests to detect cavitation in the rubber particles of a standard HIPS. Their technique is based upon a simple principle: in the absence of internal voids, the density of the rubber phase in a toughened plastic changes on application of superimposed axial stresses, thereby causing a shift in the glass transition in the rubber particles. Thus under compression the density of the rubber increases, and the secondary loss peak moves to higher temperatures. Conversely, under superimposed tension, the loss peak should shift to lower temperatures. However, all three of the HIPS materials tested by Lin et al. showed a different response to axial stress: although the low temperature  $\tan \delta$  peaks shifted upwards under compression, as expected, they were unaffected by superimposed tension, indicating that the stresses and strains in the rubber phase were independent of the large axial tensile stresses applied to the HIPS. These results clearly indicate that failure has occurred either within the rubber particle

(cavitation) or at the particle–matrix boundary (debonding), making the density of the rubber phase independent of the tensile stress applied to the HIPS specimen. Electron microscopy showed that internal cavitation with formation of rubber fibrils was responsible for this behaviour. The fibrils are stretched between neighbouring polystyrene sub-inclusions in the ‘salami’ particles, or between sub-inclusions and matrix.

Previous studies of rubber particle cavitation have been based mainly on measurements of volume strain, small-angle X-ray scattering, light scattering, electron microscopy, or other methods in which the detection of rubber particle cavitation depends upon large-scale expansion of the cavities, which may initially be less than 10 nm in diameter. Consequently, these methods provide data on the initiation and development of dilatational yielding, rather than on the cavitation event itself. A major advantage of the new dynamic mechanical technique used in the present study is that it provides a method for observing the *onset* of rubber particle cavitation as a separate process, without the complications that arise when shear yielding or multiple crazing occur at the same time.

Against this background, the paper presents dynamic mechanical data on RT-PMMA tested under superimposed static axial loading, and discusses the information about rubber particle cavitation that can be obtained from these results.

## 2. Experimental

### 2.1. Materials

The material used in this study was a transparent rubber-modified PMMA supplied by the Acrylics Division of ICI plc. It contains 40 wt% of core–shell particles, each comprising a solid PMMA core, an acrylic rubber inner shell, and a PMMA outer shell. This material provides a combination of high impact resistance, rigidity, heat resistance, and surface hardness.

### 2.2. Specimen preparation

Granules were dried for approximately 1 h in a vacuum oven before being compression moulded between chromium-plated steel sheets to form 3 mm thick plaques. A film of lubricant, Frekote Aqualine C-200 water-based releasing interface, was sprayed onto the sheets to aid polymer flow and prevent sticking. Compression moulding was carried out at  $\sim 200^\circ\text{C}$  at a nominal pressure of  $\sim 4$  MPa. The plaques were allowed to anneal by cooling from the moulding temperature to room temperature at a rate of  $\sim 0.5^\circ\text{C min}^{-1}$ .

For dynamic tests under superimposed tension, dumbbell specimens with gauge portions measuring  $3 \times 3 \times 20$  mm<sup>3</sup> were machined from the moulded sheets using a router. For tests under superimposed compression, rectangular bars

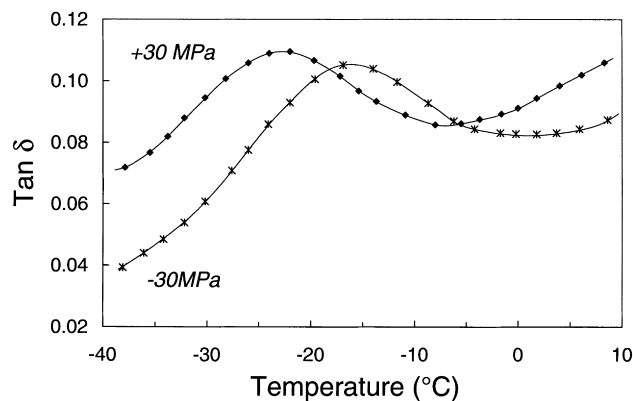


Fig. 1. Typical dynamic loss curves for specimens tested under superimposed uniaxial stresses of +30 MPa and -30 MPa.

measuring  $3 \times 3 \times 10 \text{ mm}^3$  were cut with a low speed rotary saw, using paraffin as a lubricant and coolant. Cut surfaces of machined bars were polished with fine emery cloth to avoid premature fracture in tension during testing.

### 2.3. Dynamic mechanical testing

Tests were carried out using an Eplexor dynamic mechanical thermal spectrometer (DMTS) manufactured in Germany by Gabo Qualimeter GmbH. This instrument is able to apply static loads of upto 1500 N to the specimen, in various configurations including uniaxial tension or compression, while simultaneously measuring dynamic mechanical properties at small load amplitudes.

In both tension and compression tests, static and dynamic stresses were applied to the specimens in a direction parallel to the length of the bar. Axial static loads in the range -40 MPa (compression) to +30 MPa (tension) were first applied to the specimens at 23°C and held constant during the intervals between subsequent (intermittent) dynamic mechanical measurements.

Specimens were cooled down to -60°C (well below the  $T_g$  of the rubber) at a rate of  $10^\circ\text{C min}^{-1}$ , and then heated at an average rate of  $1^\circ\text{C min}^{-1}$ . Dynamic tests were conducted at a frequency of 1 Hz over the temperature

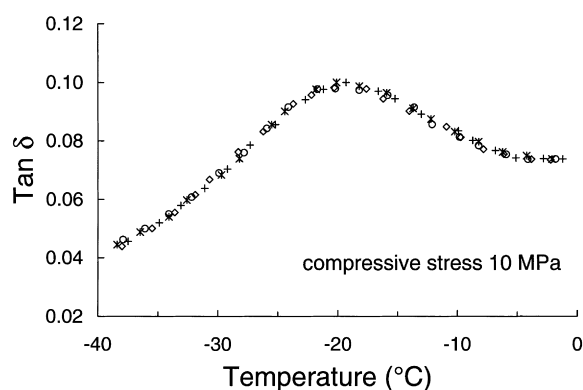


Fig. 2. Dynamic loss curves for five identical specimens, all tested under a uniaxial compressive stress of 10 MPa.

range -60 to 20°C, with a peak dynamic force of 40 N, corresponding to a dynamic strain amplitude rising from approximately  $\pm 0.1\%$  at -60°C to  $\pm 0.2\%$  at 20°C. In some preliminary tests, heating was continued to 140°C. However, the data presented below are restricted to the region of main interest, between 40 and 10°C.

### 3. Results

Preliminary dynamic mechanical measurements over a wide range of temperatures showed two distinct transitions in the RT-PMMA blend: a minor one at about -20°C, which corresponds to the  $\alpha$  (glass) transition in the acrylate copolymer rubber phase, and a major one at about +120°C, which is due to the glass transition of the PMMA matrix. The following discussion concentrates on the  $\alpha$  transition in the rubber phase, which can conveniently be characterised by the maximum in  $\tan \delta$  at temperature  $T_\alpha$ .

Fig. 1 presents typical loss curves obtained under superimposed axial stresses of -30 and +30 MPa, which clearly affect the position  $T_\alpha$  of the  $\tan \delta$  peak, but have little effect on its height or general shape. Both peaks are relatively broad, but it is nevertheless possible to define their maxima to within  $\sim 0.5^\circ\text{C}$ . In order to check the reproducibility of these measurements, at least four separate specimens were tested under each loading condition. Fig. 2 combines data obtained from four separate specimens, each tested under a compressive stress of 10 MPa, and demonstrates that both the specimens and the test equipment give very reproducible results. The same procedure was repeated at -2 MPa, and also at 5 MPa intervals from -5 to -40 MPa; in each case the same high level of reproducibility was observed. It is therefore concluded that quoting values of  $T_\alpha$  to a precision of  $0.5^\circ\text{C}$  is justifiable.

The pattern changes significantly, however, when specimens are compared under superimposed tensile stress, as illustrated in Fig. 3. The loss curves no longer coincide, and the temperature of the peak maximum varies from specimen to specimen. Similar variations were found in all six sets of curves obtained from specimens tested in tension, at +2 MPa and at 5 MPa intervals from +5 to +30 MPa. Those accustomed to analysing dynamic mechanical test data obtained using other equipment, in which specimens are subjected to little or no axial stress, might regard these variations as within experimental error, and therefore unimportant. However, in the present work the variability of curves obtained under superimposed tension is so much greater than that of curves obtained under compression that the difference can confidently be attributed to changes in the properties of the material on application of tensile stress, even at levels as low as 2 MPa.

In order to characterise this change in behaviour, dynamic loss data for different specimens, all tested at the same superimposed stress level, were compared at three selected temperatures: -40, -20 and 0°C. The reason for choosing

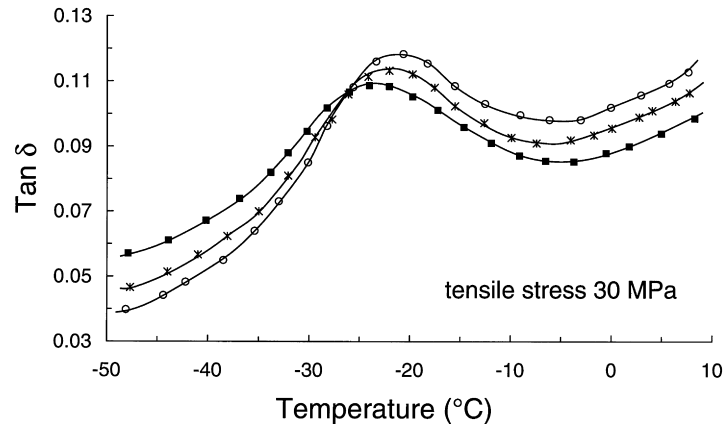


Fig. 3. Dynamic loss curves for three identical specimens, all tested under an uniaxial tensile stress of 30 MPa.

these temperatures is that  $-20^{\circ}\text{C}$  is close to  $T_{\alpha}$  for all specimens, although in only a few cases does  $T_{\alpha}$  lie exactly at  $-20^{\circ}\text{C}$ . The results of this comparison are illustrated in Fig. 4, which records the distribution of  $\tan \delta$  values obtained at each applied stress, based in each case on sets of at least five specimens in tension and four in compression. For each set, the lowest value of  $\tan \delta$  at the chosen test temperature is subtracted from  $\tan \delta$  (for specimen  $i$ , where  $i$  takes all values from 1 to 4 (in compression) or 5 (in tension), and therefore includes the specimen with the lowest  $\tan \delta$ ). This method of presentation emphasises the contrast in dynamic mechanical behaviour between specimens tested in compression and specimens tested in tension.

In a few cases, application of a tensile stress caused the loss peak to split into two, as illustrated in Fig. 5, where the maxima are  $4^{\circ}\text{C}$  apart. This splitting is similar to that reported by Morbitzer et al. in ABS [5,6], and clearly reflects the presence of two distinct populations of rubber particles, exhibiting different levels of cavitation, and therefore different stresses and strains in the rubber phase.

Data from all of the tests carried out during this study are compared in Fig. 6, which plots the temperature of the  $\tan \delta$

peak against superimposed axial stress. For tests carried out under compression, the trend is very clear, and similar to that observed by Lin et al. in HIPS: the peak shifts to higher temperatures as the applied (negative) stress is increased, because the density of the rubber phase increases. However, the data from tests carried out under tension present a more complicated picture. Some points from tests at  $+2$  to  $+10$  MPa fit neatly onto the extrapolated curve through the compression data, but most are clearly above that curve, some by as much as 8 K. For any given tensile stress, the greatest separation between measured values of  $T_{\alpha}$  is 6 K. As noted earlier, peak separations of similar magnitude can occur even in a single loss curve.

These results are far more comprehensive than those reported by Lin et al., and have revealed some new patterns of behaviour. The increase in variability of the dynamic loss data on changing from compression to tension is especially striking, and is in sharp contrast to the consistency observed in loss curves for HIPS under tensile loading: for all three HIPS materials tested,  $T_{\alpha}$  was independent of tensile stress, with no indication of specimen-to-specimen variability.

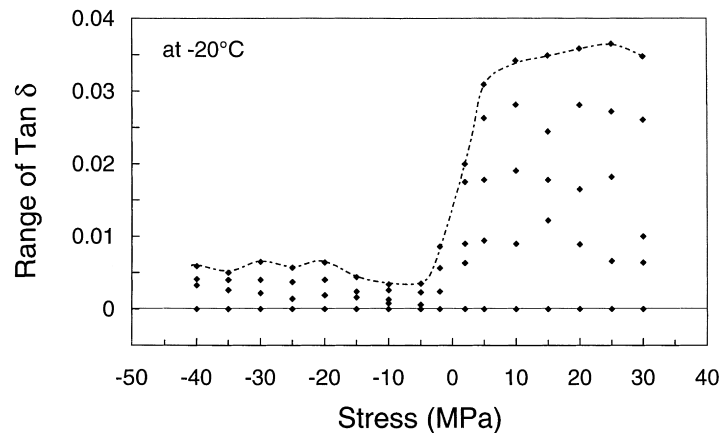


Fig. 4. Effects of superimposed static stresses upon the variability of the loss peak, expressed as the difference between the highest and lowest values of  $\tan \delta$ , in sets consisting of five specimens each, at  $-20^{\circ}\text{C}$ .

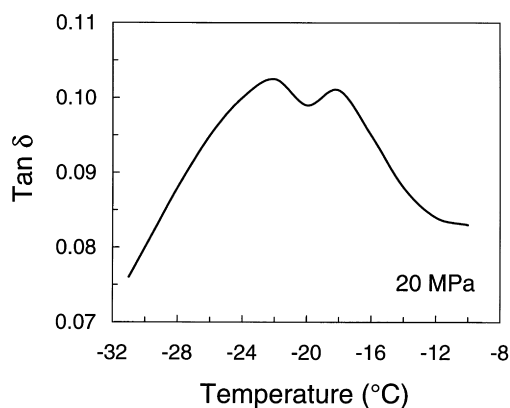


Fig. 5. Splitting of the low temperature loss peak under a superimposed axial tensile loading of 20 MPa.

#### 4. Discussion

The dynamic mechanical data reported in this paper demonstrate the way in which local stresses and strains within a standard RT-PMMA can affect the relaxation behaviour of the acrylate copolymer rubber phase, which undergoes a glass transition at about  $-20^{\circ}\text{C}$ . Observations of the corresponding low temperature loss peak show that there is a considerable degree of uniformity in specimens tested under superimposed compression, with high levels of reproducibility from specimen to specimen, and loss peak maxima shifting systematically to higher temperatures as the compressive stress is increased. This is very much as one would expect. Even if the particles all cavitated on cooling from  $100^{\circ}\text{C}$ , in the absence of an applied stress, the voids would eventually close up when pressure was applied, and relaxation times would then increase as the density increased. Fig. 6 shows a shift of  $+4^{\circ}\text{C}$  on increasing the compressive stress from 5 to 35 MPa, which corresponds to an increase of 10 MPa in the ‘hydrostatic’ pressure (negative mean stress) acting on the RT-PMMA, which by definition is one third of the uniaxial compression stress. These results may be compared with the data of

McKinney et al. [12] on vulcanised natural rubber, which show an upward shift of  $28^{\circ}\text{C}$  in the loss compliance peak on application of 981 bar (98.1 MPa) pressure. However, it must be remembered that in RT-PMMA the rubber particles are partly shielded by the rigid matrix from the effects of applied compressive stress.

In order to understand the complex relationship between applied mean stress (or ‘hydrostatic tension’) and observed loss peak temperatures, especially under tensile loading, it is helpful to employ a schematic diagram comparing the relaxation behaviour of intact rubber particles (i.e. void-free core-shell particles) with that of the bulk rubber, as in Fig. 7. Point A defines the loss peak temperature  $T_{\alpha}$  of the unstressed bulk rubber, which is higher than its true  $T_g$  because of the dynamic nature of the test. From both theoretical considerations and the work of Morbitzer [5,6], it is known that tensile stresses developed within the rubber particles as a result of constrained thermal contraction can reduce the observed loss peak temperature by as much as 20 K, and that the extent of the shift is greatest when the concentrations of rubber particles are small, hence the positions of points B and C below point A on the diagram. The constraining effect of the matrix on thermal contraction in the rubber particles becomes larger as the rubber content is reduced.

The lines through points A, B and C in Fig. 7 are based on the present work and that of McKinney [12]. From their relative positions, it can be seen that quite high ‘hydrostatic’ pressures, in the order of 20–30 MPa (equivalent to uniaxial compressive stresses of 60–90 MPa) must be applied to rubber-toughened plastics simply to reduce the mean stress in the rubber phase to zero, and thus shift the  $\tan \delta$  peak to the same temperature as point A. More generally, it can be seen that the large dilatational stresses generated in the rubber particles during cooling cause the whole  $T_{\alpha}$  vs mean stress curve to shift progressively to the left as the rubber content is decreased. In other words, if loss peak temperatures were plotted against the mean stress within the rubber particles, rather than the mean stress applied to

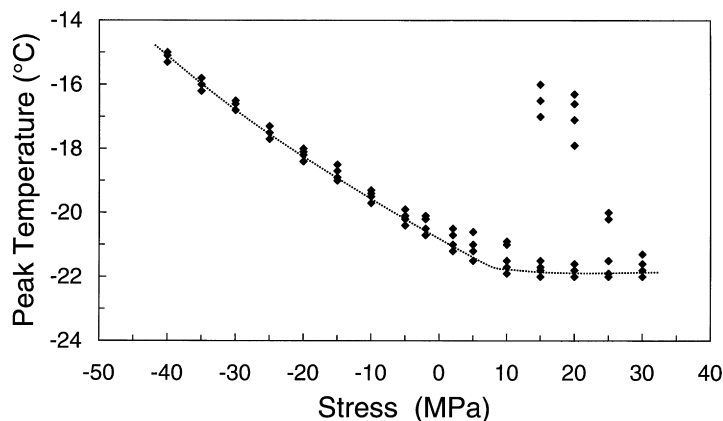


Fig. 6. Effects of superimposed uniaxial stress upon the temperatures of the secondary loss peaks in RT-PMMA. This figure summarizes data taken from a large number of dynamic mechanical tests at 1 Hz, including those represented in Figs. 1–3. Both peaks from Fig. 5 are also included.

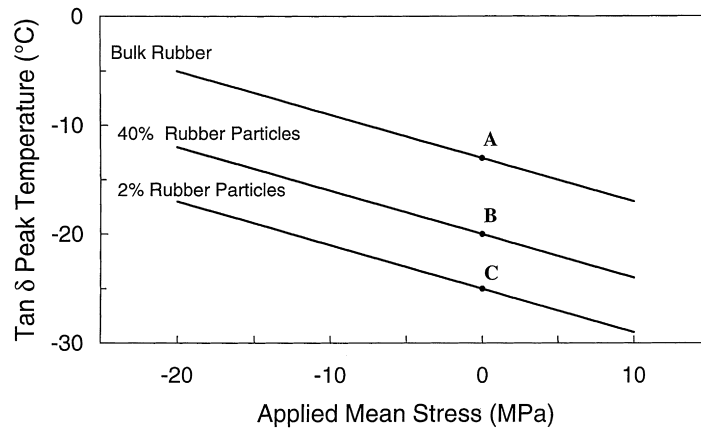


Fig. 7. Schematic diagram showing the relationship between applied mean stress and loss peak temperature for bulk rubber and for toughened polymers containing 40 and 2% rubber particles. Note that the mean ('hydrostatic') stress is one third of the uniaxial stress.

the toughened polymer, then  $T_{\alpha}$  vs mean stress curves for all rubber contents would pass through point A, and superimpose upon the curve for the bulk rubber.

An alternative way of reducing or eliminating tensile mean stresses in the rubber phase is to induce cavitation. As illustrated schematically in Fig. 8, if the particles then become fully relaxed, they will produce a  $\tan \delta$  peak at the same temperature as point A, which does not shift when the toughened polymer is subjected to tensile mean stresses (or to modest levels of compressive mean stress). If cavitation does not result in complete relaxation, the  $\tan \delta$  peak will occur at a lower temperature, as shown schematically by the lower dotted line. In Fig. 8, this second line is drawn horizontally, but it is quite possible for the residual mean stress in the rubber phase to vary with applied stress.

In the case of the chosen RT-PMMA, there is a third possibility. The presence of a solid PMMA core in each particle results in the formation of rubber fibrils, which are stretched out between core and outer shell, and therefore subject to quite high strains [13], although the mean stresses in the fibrils may be relatively small. The literature contains little information about the effects of large tensile strains on

the relaxation behaviour of rubber, but a recent study at Cranfield on vulcanised butyl rubber has shown a strong dependence of  $T_{\alpha}$  on tensile strain, as shown in Fig. 9 [14]. On the basis of this evidence, it is clear that  $T_{\alpha}$  for cavitated rubber particles can fall well below point A, because of large tensile strains in the fibrils, although mean stresses may be quite low (of order 1 MPa). The solid line marked 'Fully Stretched' in Fig. 8 represents this state. Failure of the fibrils will, of course, limit the extent of the downward shift in  $T_{\alpha}$ . The direct conversion of intact rubber membranes to highly stretched fibrils would explain the data reported by Lin et al. for HIPS [11], and would be consistent with transmission electron microscope observations.

Applying these principles to Fig. 6, it can be seen that point B, at which zero axial stress is applied to RT-PMMA, corresponds to a loss peak temperature of  $-21^{\circ}\text{C}$ . Because of differential thermal contraction from  $+120^{\circ}\text{C}$ , the rubber phase is in triaxial tension at this point, and  $T_{\alpha}$  for the fully relaxed rubber must therefore be substantially higher than  $-21^{\circ}\text{C}$ . Taking reasonable values for the moduli and expansion coefficients of the rubber and PMMA phases, and

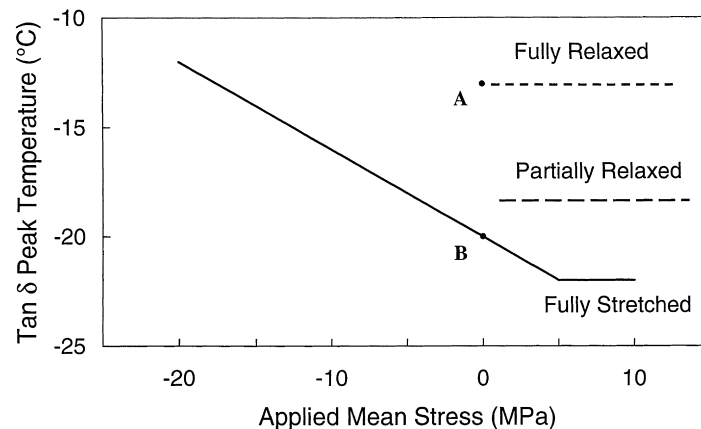


Fig. 8. Schematic diagram showing the effects of rubber particle cavitation upon loss peak temperature, where the cavitated rubber is (a) fully relaxed; (b) partially relaxed; and (c) fibrillated and highly stretched.

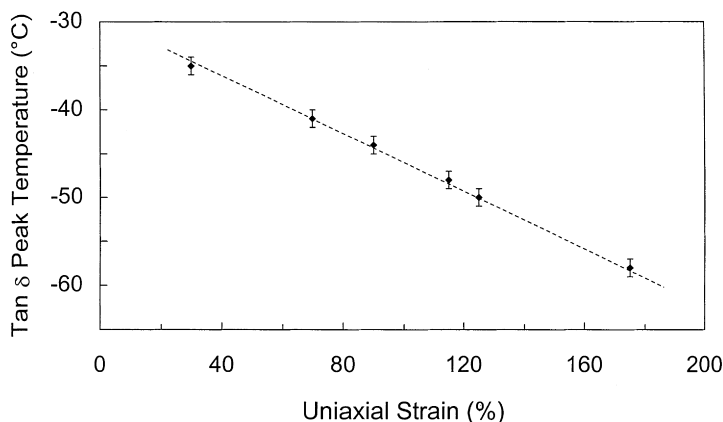


Fig. 9. Relationship between loss peak temperature and tensile strain for vulcanised butyl rubber (from Ref. [14]).

assuming that there is no stress relaxation on cooling to  $-20^{\circ}\text{C}$ , calculations give a maximum value of +3% for the volume strain in the rubber phase, in the absence of applied stress. At this volume strain, the loss peak temperature for intact rubber particles should be about  $11^{\circ}\text{C}$  below that of the fully relaxed rubber. In other words, the estimated temperature at point A on the diagram is  $-10^{\circ}\text{C}$ .

It follows that the observed loss peak temperature could rise as high as  $-10^{\circ}\text{C}$  once the rubber particles have cavitated, assuming that the stresses and strains in the rubber phase fall to zero at that stage. This assumption is reasonable for some rubber-toughened plastics, but is not necessarily valid for the RT-PMMA under investigation, because of its morphology. As in all transparent grades of RT-PMMA, the rubber is present as a spherical inner shell which lies between a concentric spherical core of PMMA and an outer shell of PMMA, to both of which it is securely grafted. The outer PMMA shell binds the particle firmly to the surrounding matrix. Consequently, on cavitation the elastomeric shell tends to break up into fibrils, which connect the rigid core to the rigid matrix [13], in a similar manner to that observed in HIPS. During the early stages of cavitation, when total volume strains in the rubber particle are still in the order of 1%, only part of each elastomeric shell may be affected, with the remainder forming an intact layer connecting the core to the matrix. However, as the strain in the neighbouring matrix increases, and especially if it begins to craze, the volume strain in the particle will increase, and fibrillation of the rubber phase will spread until the whole of the shell is affected [13].

In the light of the foregoing discussion, it becomes a little clearer why the dynamic mechanical behaviour of RT-PMMA is so variable when static tensile stresses are superimposed upon the dynamic loads required for the measurements. Once the stored elastic energy becomes large enough to generate voids in the rubbery shells of the particles, the acrylic elastomer may be found in one of at least three states: (a) material that has fibrillated and stretched to moderate or high strains (extensions up to  $\sim 400\%$ ) [13]; (b) intact (i.e. void-free) regions that are

partially relaxed because cavitation has occurred elsewhere in the particle, and has thus redistributed the thermally generated volume strains; and (c) rubber that is intact and unrelaxed, because no cavitation has occurred anywhere in the particle. Partial relaxation of volume strains within intact particles is also possible, as a result of cavitation in neighbouring particles.

Large extensions can have profound effects upon the relaxation behaviour of elastomers. To date, it has not been possible to obtain specimens that are suitable for studying these effects in acrylate copolymer rubbers, but experiments on vulcanised butyl rubbers show downward shifts of as much as  $-25^{\circ}\text{C}$  on increasing the tensile (engineering) strain from 30 to 175%, as illustrated in Fig. 9 [14]. These results suggest that in Fig. 6 the series of peaks grouped around  $-22^{\circ}\text{C}$ , especially at higher tensile stresses, could be due to fibrils of rubber that are stretched between core and matrix, and are approaching breaking point. According to this interpretation, the peaks at about  $-16^{\circ}\text{C}$  in specimens subjected to 15 or 20 MPa tensile stress are due either to less highly stretched fibrils or to partially relaxed intact rubber layers in partially cavitated shells. The total volume of intact rubber regions of this kind in any given specimen will necessarily decrease as overall tensile strains increase, thereby increasing the local volume strains in individual particles, so that fibrillation spreads throughout the material.

This study has demonstrated the effectiveness of the novel dynamic mechanical technique in detecting the onset of rubber particle cavitation in rubber-toughened plastics, thus confirming the earlier conclusions reached by Lin et al. [11]. In the RT-PMMA grade chosen for the present study, the transition occurs at imposed stresses between  $-2$  and  $+2$  MPa, which are too small to cause significant shear yielding or crazing: at a temperature of  $-10^{\circ}\text{C}$ , the tensile yield stress of the RT-PMMA is  $\sim 50$  MPa.

Another important result of this work is that the technique can be used to detect distributions of stress and strain within the rubber phase after the onset of cavitation in the particles. This method could provide valuable information

about the progress of cavitation under increasing applied loads.

## 5. Conclusions

This work has shown that cavitation of the rubber particles can be detected and monitored in toughened plastics using dynamic mechanical thermal spectroscopy of specimens subjected to a range of compressive and tensile axial stresses. In the RT-PMMA studied, the onset of cavitation occurs at axial stresses close to zero, and must therefore be largely due to internal stresses generated by differential thermal contraction. Calculations show that the tensile mean stress (negative pressure) developed in the rubber shell at  $-20^{\circ}\text{C}$  could be as high as 60 MPa, corresponding to a volume strain of about +3%. A dilatation of this magnitude should cause a downward shift of about 11 K in the glass transition temperature of the rubber phase, which is reversed when the rubber cavitates. Subsequent fibrillation and stretching of the rubber phase has the opposite effect, of depressing the transition temperature  $T_{\alpha}$ . As a result of these competing influences on the relaxation behaviour of the rubber phase, and the distribution of stresses and strains within and between rubber particles once cavitation has begun, there is a considerable specimen-to-specimen variation in the data obtained from dynamic mechanical tests under superimposed tension. By contrast, tests under compressive loading show excellent reproducibility, with  $T_{\alpha}$  increasing approximately linearly with increasing compressive stress.

The dynamic mechanical technique described in this paper shows great promise as a method for investigating the role of rubber particles in toughening of thermoplastics and thermosetting resins.

## Acknowledgements

The authors thank the Acrylics Division of ICI plc for their support of this research program, and for permission to publish this paper. They also thank EPSRC for grant GR/K99824 towards the purchase of the Gabo dynamic mechanical spectrometer, and the following companies for their additional contributions to the cost of the equipment: BASF, DSM, Gearing Scientific, ICI plc, London International, and Short Brothers.

## References

- [1] Bucknall CB. In: Haward RN, Young RJ, editors. The physics of glassy polymers, 2. London: Chapman & Hall, 1997.
- [2] Bucknall CB. In: Paul DR, Bucknall CB, editors. Polymer blends: formulation and performance, New York: Wiley, 2000 chap. 22.
- [3] Yang HH, Bucknall CB. 10th International Conference on Deformation, Yield and Fracture of Polymers, Cambridge 7–10 April 1997, Institute of Materials, London.
- [4] Ayre DS, Bucknall CB. *Polymer* 1998;39:4785.
- [5] Humme G, Kranz D, Morbitzer L, Ott KH. *J Appl Polym Sci* 1976;20:2691.
- [6] Morbitzer L, Humme G, Ott KH, Zabrocki K. *Angew Makromol Chem* 1982;108:123.
- [7] Lazzeri A, Bucknall CB. *J Mater Sci* 1993;28:6799.
- [8] Bucknall CB, Karpodinis A, Zhang XC. *J Mater Sci* 1994;29:3377.
- [9] Lazzeri A, Bucknall CB. *Polymer* 1995;36:2895.
- [10] Bucknall CB, Ayre DA, Dijkstra DJ. Submitted for publication.
- [11] Lin CS, Ayre DS, Bucknall CB. *J Mater Sci Lett* 1998;17:669.
- [12] McKinney JE, Belcher HV, Marvin RS. *Trans Soc Rheol* 1960;4:347.
- [13] Starke JU, Godehardt R, Michler GH, Bucknall CB. *J Mater Sci* 1997;32:1855.
- [14] Bucknall CB, Rizzieri R. In preparation.